

# Journal of Materials Chemistry B

Accepted Manuscript



This is an *Accepted Manuscript*, which has been through the Royal Society of Chemistry peer review process and has been accepted for publication.

*Accepted Manuscripts* are published online shortly after acceptance, before technical editing, formatting and proof reading. Using this free service, authors can make their results available to the community, in citable form, before we publish the edited article. We will replace this *Accepted Manuscript* with the edited and formatted *Advance Article* as soon as it is available.

You can find more information about *Accepted Manuscripts* in the [Information for Authors](#).

Please note that technical editing may introduce minor changes to the text and/or graphics, which may alter content. The journal's standard [Terms & Conditions](#) and the [Ethical guidelines](#) still apply. In no event shall the Royal Society of Chemistry be held responsible for any errors or omissions in this *Accepted Manuscript* or any consequences arising from the use of any information it contains.

## Internal Polymer Scaffolding in Lipid-Coated Microbubbles for Control of Inertial Cavitation in Ultrasound Theranostics

 Shih-Tsung Kang<sup>a</sup>, Jian-Liang Lin<sup>a</sup>, Chung-Hsin Wang<sup>a</sup>, Yuan-Chih Chang<sup>b</sup>, and Chih-Kuang Yeh<sup>a,\*</sup>

 Received 00th January 20xx,  
 Accepted 00th January 20xx

DOI: 10.1039/x0xx00000x

www.rsc.org/

**A lipid-polymer composite structure was developed for tuning of inertial cavitation activity of microbubbles under ultrasound exposure. The incorporation of a thin layer of polymer networks inside the lipid monolayer resulted in a marked reduction in inertial cavitation dose. This strategy is potential to increase the safety of ultrasound theranostic applications assisted by microbubble cavitation.**

Advances in ultrasound drug delivery technologies have extended the use of microbubbles (MBs) contrast agents from conventional ultrasound imaging to ultrasound theranostics.<sup>1,2</sup> MBs have a highly hydrophobic gas core (e.g., SF<sub>6</sub>, C<sub>3</sub>F<sub>8</sub>, or C<sub>4</sub>F<sub>10</sub>) stabilized by a shell of phospholipids, albumin, or polymers. They can carry drug molecules, DNA fragments, or nanoparticles.<sup>3</sup> Mild oscillation of MBs has been shown to generate nonlinear ultrasound echoes for contrast-enhanced ultrasound imaging.<sup>4</sup> It also produces forces responsible for release of drug payloads and temporary permeabilization of neighboring tissues,<sup>5,6</sup> which are beneficial in the treatments of tissues bearing a blood-tissue barrier (such as in brain and retina) or suffering low vascularity (such as solid tumors).<sup>7-9</sup> However, violent oscillation of MBs has been shown to cause side effects such as cell death and capillary hemorrhage,<sup>10,11</sup> resulting in the major obstacles for clinical use of MBs in cavitation-assisted diagnosis and therapy.

Stable and inertial cavitation are the two regimes classifying the mild and violent oscillation of MBs, respectively. In the stable cavitation regime, MBs undergo sustained pulsation to generate nonlinear harmonic echoes with multiples or submultiples of the driving ultrasound frequency.<sup>3</sup> The resulting mild mechanical forces and microstreaming are capable of inducing cell membrane damage recoverable in a few minutes.<sup>12</sup> When entering the inertial cavitation regime at higher pressures, MBs exhibit much higher amplitudes of pulsation and inertial collapse with velocities of up to hundreds of meters per second and may end up being disrupted in

a few cycles.<sup>13</sup> The resulting strong microstreaming, shock waves, and impact jetting have been shown to cause irreversible cell membrane perforation and vessel rupture.<sup>12</sup> Although both the regimes have reportedly contributed to successful *in vitro* or *in vivo* ultrasound contrast imaging and drug delivery,<sup>3,14</sup> the induction of inertial cavitation should be avoided in biological tissues that are vulnerable to hemorrhage-related side effects, particularly in brain.<sup>11</sup> However, establishing optimal ultrasound settings capable of inducing stable cavitation but suppressing inertial cavitation is challenging, since the transition between these two regimes takes place in a short pressure range of only a few hundreds of kilopascals. Considering both ultrasound frequency and pressure amplitude, the transition range can be categorized in terms of mechanical index to be 0.2–0.5.<sup>3,15</sup> Hence, it is preferable to use MBs with a lower ability to undergo inertial cavitation in order to compensate unpredictable ultrasound field distortion due to the complexity in the *in vivo* environment.

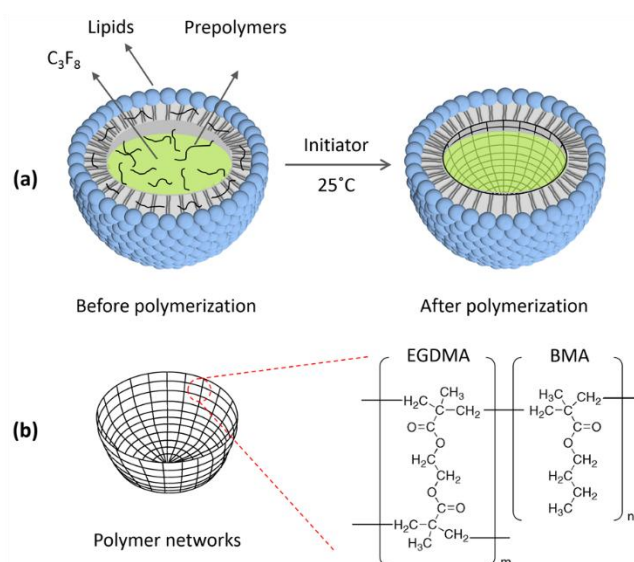


Fig. 1. Schematic diagrams for the formation of a thin layer of polymer networks in LP-MBs. (a) Structural difference of LP-MBs before and after internal polymer network formation. (b) Hypothesized structure of polymer networks composed of hydrophobic prepolymers (EGDMA and BMA) inside the lipid monolayer of LP-MBs.

<sup>a</sup> Department of Biomedical Engineering and Environmental Sciences, National Tsing Hua University, Taiwan. E-mail: ckyeh@mx.nthu.edu.tw.

<sup>b</sup> Institute of Cellular and Organismic Biology, Academia Sinica, Taiwan.

† Electronic Supplementary Information (ESI) available: [Experimental details, Table S1, and Fig. S1–S4]. See DOI: 10.1039/x0xx00000x

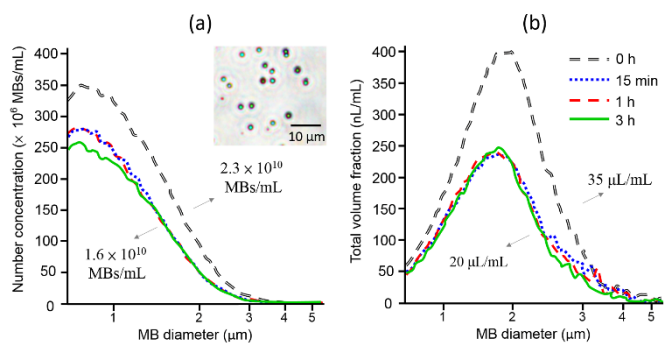


Fig. 2. Size distributions of LP-MBs subjected to 0–3 h of polymerization: (a) number concentration and (b) total volume fraction as a function of MB diameter. The inset picture in (a) shows the bright-field microscopy images of 3-h polymerized LP-MBs.

To date, few techniques have been proposed for suppression of inertial cavitation, such as stabilizing MBs with a stiff polymer or albumin shell, or nesting lipid-coated MBs in the aqueous core of a polymer microcapsule.<sup>16–18</sup> However, these predictably compromise the performance of MBs to generate ultrasound echoes and exert bioeffects with stable cavitation in the therapeutic frequency range of 1–10 MHz. Stiffer shells lead to higher frequencies and higher threshold pressures for induction of MB resonance.<sup>19</sup> Increasing the mole fraction of poly (ethylene glycol) (PEG) on lipid-stabilized MBs from 5% to 10% has also been shown to reduce inertial cavitation by moderately modifying the interfacial rheology, but the mole fractions of PEG higher than 10% have been reported to increase the shell stiffness and decrease the stability of MBs.<sup>20,21</sup>

Herein, we developed lipid-polymer composite MBs (LP-MBs) as an alternative strategy for tuning of inertial cavitation. A thin layer of polymer networks was woven in the interior of template MBs which possessed a preformed gas body and a densely packed lipid monolayer (Fig. 1a). The thin network structure was presumed to serve as a supported scaffold to hinder the violent expansion and inertial collapse of MBs with minimum influence on the stable oscillation of MBs under ultrasound exposure. The outer lipid shell preserves the advantages such as high biocompatibility, low toxicity, and low immunogenicity.<sup>22</sup> To test this hypothesis, hydrophobic prepolymers (including monomers and crosslinkers) were embedded in the lipid monolayer of MBs for production of crosslinking polymer networks (Fig. 1b). The morphological properties of LP-MBs after subjected to different polymerization durations were characterized to validate the presence of polymer networks. The effects of the internal polymer scaffolding on the stability and cavitation properties of LP-MBs were investigated by assessing *in vitro* stability against dilution, *in vivo* ultrasound contrast persistence, and stable and inertial cavitation doses at different ultrasound pressures.

Lipids (2-distearoyl-sn-glycero-3-phosphocholine, DSPC, and methoxypoly(ethylene glycol)distearoyl-phosphatidyl ethanolamine, DSPE-PEG2000), monomers (butyl methacrylate, BMA) and crosslinkers (ethylene glycol dimethacrylate, EGDMA) were used to formulate LP-MBs. In brief, a homogenous mixture of these materials was dispersed in PBS by sonication, and was sealed in a 2-mL vial filled with perfluoropropane ( $C_3F_8$ ) gas. Afterward, the vial was subjected to intense agitation for 45 s to form template LP-MBs. Crosslinking of BMA and EGDMA inside LP-MBs was triggered by the

addition of initiator (ammonium persulfate, APS) and accelerator (tetramethylethylenediamine, TEMED) for induction of radical polymerization. To ensure homogeneity, the polymerization was run under gentle stirring for different durations (for 3 h unless otherwise specified) at room temperature. Polymerized LP-MBs were purified for removal of free lipids and prepolymers that failed to encapsulate  $C_3F_8$  and excess APS and TEMED to terminate the polymerization process. Detailed experimental procedures were included in the ESI.

To determine whether the formation of crosslinking polymer networks influences the morphology of LP-MBs, Coulter principle-based particle sizing (Multisizer 3, Beckman Coulter, FL, USA), cryogenic transmission electron microscopy (Cryo-TEM) (Tecnai G2 F20, FEI, OR, USA), and negative-stain TEM (HT7700, Hitachi, IL, USA) were conducted to characterize the size and structural changes of LP-MBs before and after the internal polymerization. The results of the size measurements indicated that the copolymerization of EGDMA and BMA did not influence the size distributions of LP-MBs (Fig. 2a,b). Polymerized (15 min, 1h, and 3 h) and nonpolymerized (0 h) LP-MBs had similar polydisperse size distributions with a mean diameter of 1.2  $\mu\text{m}$  and a peak diameter of 0.7  $\mu\text{m}$ . The small reductions in number concentration and total volume fraction were caused by the gentle stirring. Nevertheless, the high concentration of  $C_3F_8$  in the sealed vials had driven the polymerized LP-MBs to reach an equilibrium state of gas exchange, resulting in no further losses of MBs with increasing polymerization time. The results of the Cryo-TEM have confirmed the formation of polymer networks in LP-MBs subjected to 3 h of polymerization. The basic structure of LP-MBs appeared as a bright hollow gas core of  $C_3F_8$  circled by a dark layer composed of densely packed DSPC

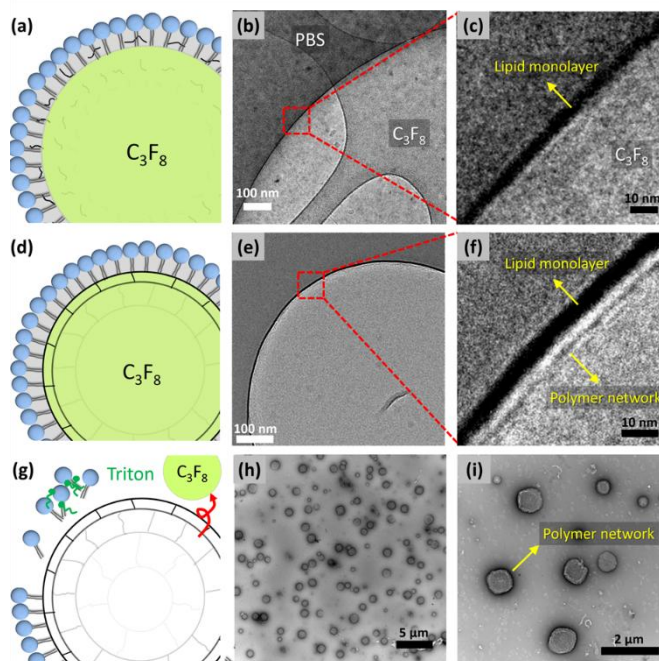


Fig. 3. Morphological properties of LP-MBs before and after polymerization. (a–f) Schematic diagrams and corresponding Cryo-TEM images of LP-MBs in the cross-sectional view for polymerization duration of 0 h (a–c) and 3 h (d–f). (g–i) Schematic diagram and corresponding negative-stain TEM images of extracted polymer networks in 3-h polymerized LP-MBs after removal of lipid coatings by Triton X-100.

and DSPE-PEG2000. Before 3 h of polymerization, EGDMA and BMA were presumably intercalated within lipids in the absence of an independent structure (Fig. 3a–c). After 3 h of polymerization, the intercalated EGDMA and BMA were interconnected to form a thin layer of polymerized networks distinguishable in the interior of the lipid layer (Fig. 3d–f). The layer had a thickness of about 1 nm, which was much thinner than the outer lipid layer (~3 nm). This may be attributed to the limited loading capacity of the lipid layer for the prepolymers. To further confirm the integrity of the polymer networks without the support of lipids, the polymerized LP-MBs were disrupted by removal of lipids under a sonication bath after addition of 1% Triton X-100. The images of negative-stain TEM conducted with 1% of uranyl acetate showed the intact spherical leftovers of polymer networks with diameters of 0.7–1.2  $\mu\text{m}$  (Fig. 3g–i). The good agreement with the size measurements results provided the evidence of polymer network formation in the polymerized LP-MBs.

To determine whether the layer of polymer networks reduced the stability of LP-MBs, polymerized (3 h) and nonpolymerized (0 h) LP-MBs were diluted to a total volume fraction of 10 nL/mL in isotonic saline, and subsequently maintained at 37°C for up to 3 h for quantification of the change in the total volume fraction of MBs as a function of time. An *in vitro* half-life was defined as the time taken for a 50% decrease in the total volume fraction of MBs. The results indicated that the *in vitro* half-life of LP-MBs with 3-h polymerization was about 60 min ( $N = 5$ ), which was 30 min shorter than those without polymerization (ESI Fig. S1). Despite the shorter *in vitro* half-life, polymerized LP-MBs were found to be as stable as nonpolymerized LP-MBs in the first 20 min with no detectable loss. This duration has exceeded the time reported for the complete *in vivo* clearance of clinically available MBs agents (e.g., Definity® and

SonoVue®) by lung, liver, and spleen. Hence, polymerized LP-MBs were assumed to provide *in vivo* ultrasound contrast persistence comparable with that of nonpolymerized LP-MBs. As validated by the results of ultrasound brain imaging in rats (ESI Fig. S2), the ultrasound contrast enhancements in the dorsal sagittal sinus of both polymerized and nonpolymerized LP-MBs rapidly increased to 20 dB after MB injection; they slowly decreased at the same decay rate, and did not return to the background level after 10 min. The circulation persistence suggested the suitability of polymerized LP-MBs for *in vivo* use.

To validate the effect of internal polymer scaffolding on the cavitation properties of LP-MBs, the abilities of polymerized and nonpolymerized LP-MBs to undergo stable and inertial cavitation were tested under single-pulse ultrasound exposure (10 MHz and 100 cycles) with different ultrasound pressures. The experiments were conducted in a passive cavitation detection setting (ESI Fig. S4) for acquisition of pure ultrasound signals scattered from oscillating MBs. The acquired signals possessed distinct spectral characteristics that can be used to quantify the degrees of stable and inertial cavitation. The results of the spectral analysis showed the generation of a narrow subharmonic peak at 5 MHz at 900 kPa, followed by pronounced spectral broadening at 1400 kPa (Fig. 4a–c). These were indicative of the stable resonance and inertial collapse, respectively, of LP-MBs, and their area under the curves (depicted in gray) were used to calculate stable and inertial cavitation doses, respectively. The statistical results indicated that stable and inertial cavitation doses increased with increasing ultrasound pressure at above different thresholds of 800 and 1000 kPa, respectively (Fig. 4d,e). Notably, a pronounced decrease in the inertial cavitation dose, but not the stable cavitation dose, was observed between polymerized and nonpolymerized LP-MBs; the difference increased

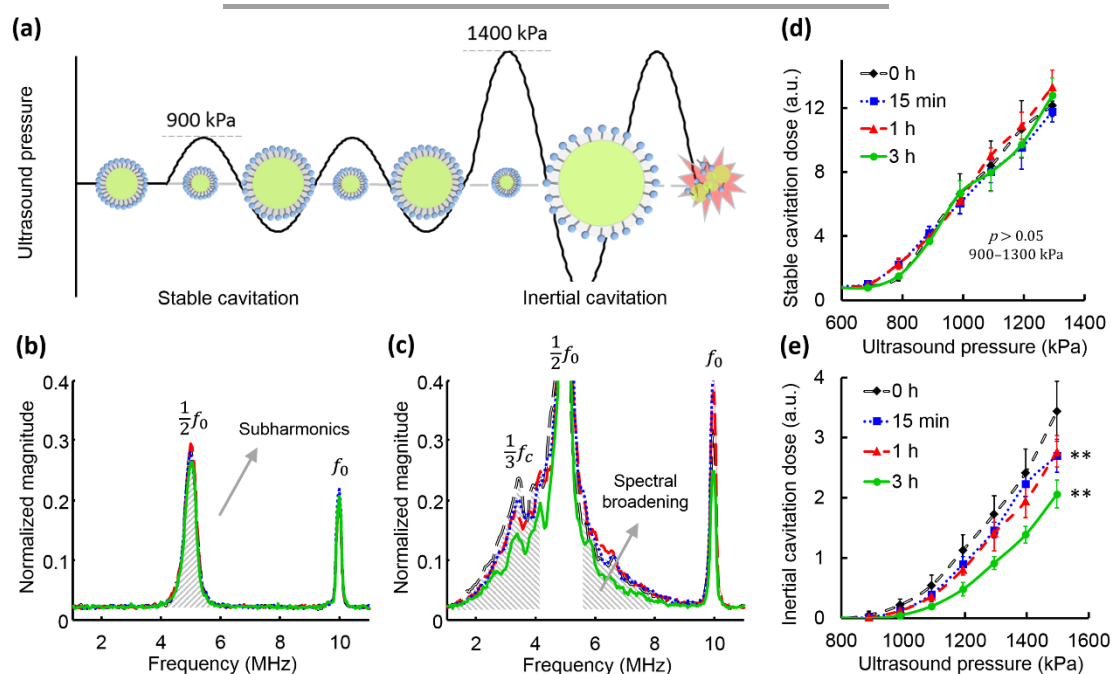


Fig. 4. Cavitation properties of LP-MBs before and after polymerization. (a) Schematic diagram of MB in stable and inertial cavitation regimes. (b,c) Spectral analysis of scattered ultrasound signals from LP-MBs under ultrasound exposure (10 MHz and 100 cycles) with pressure amplitudes of 900 kPa (b) and 1400 kPa (c) for different polymerization durations of 0–3 h. Stable cavitation (d) and inertial cavitation (e) doses of LP-MBs as a function of ultrasound pressure for polymerization durations of 0–3 h ( $N = 5$ ).

with increasing polymerization duration by up to 30% at 1500 kPa ( $p < 0.01$ ). This indicated that the higher degree of polymerization resulted in the lower ability of LP-MBs to undergo inertial cavitation with no compromise in the ability of LP-MBs to undergo stable cavitation. The suppression of inertial cavitation activity was not caused by the change of acoustic resonance properties since LP-MBs polymerized for different times were found to have consistent resonance frequency distributions (ESI Fig. S3), which were determined by the frequency-dependent attenuation of through-transmission ultrasound signals due to MB resonance.

The results have shown that the incorporation of a thin layer of polymer networks in the lipid monolayer resulted in consistent stable cavitation activity but suppressed inertial cavitation activity of polymerized LP-MBs. The mechanism may be attributed to the decrease in the amplitude of violent MB expansion and collapse. It can be observed from the suppression of high-order subharmonic signals at one-third the driving frequency (~3.5 MHz) arising from repeated inertial cavitation events (Fig. 4c).<sup>23</sup> Considering the high consistency in the resonance frequency distributions and the stable cavitation activities of the different LP-MB samples, we speculated that the effects of the internal polymerization on the shell rheology of MBs were not involved with the change in shell elasticity (which reportedly alters acoustic resonance frequency of MBs), but with the increase in shell viscosity.<sup>19</sup> Although the incorporated polymer networks was not covalently connected to the lipid layer, they were in close contact with the lipid layer via hydrophobic interactions. The contact force might have restricted lateral lipid trafficking and thus resulted in increased friction on the lipid layer to damp violent MB oscillation. The higher degree of polymerization would enhance the contact force due to the higher crosslinking density and lower membrane fluidity.

In conclusion, the incorporation of a thin and soft crosslinking polymer network as a scaffold for the lipid shell of MBs can serve as an effective strategy for tuning of inertial cavitation activity by damping MB oscillation amplitude. Inertial collapse reportedly responsible for ultrasound mechanical bioeffects may be suppressed, rendering LP-MBs potential for use in cavitation-assisted ultrasound contrast imaging and drug delivery.

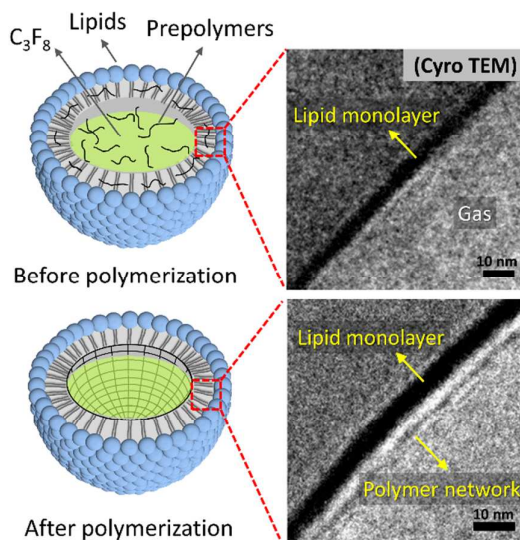
The authors gratefully acknowledge the support of the Ministry of Science and Technology, Taiwan under Grant No. 102-2221-E-007-020-MY3, National Tsing Hua University (Hsinchu, Taiwan) under Grant No. 104N2046E1, and Chang Gung Memorial Hospital (Linkou, Taiwan) under Grant No. CIRPD2E0051.

## Notes and references

- 1 S. T. Kang and C. K. Yeh, *Biomed. J.*, 2012, **35**, 125-139.
- 2 H. L. Liu, C. H. Fan, C. Y. Ting and C. K. Yeh, *Theranostics*, 2014, **4**, 432.
- 3 K. Kooiman, H. J. Vos, M. Versluis and N. de Jong, *Adv Drug Deliver Rev*, 2014, **72**, 28.
- 4 M. L. Li, Y. C. Kuo and C. K. Yeh, *Ultrasound Med. Biol.*, 2010, **36**, 1535.
- 5 Y. Luan, G. Lajoinie, E. Gelderblom, I. Skachkov, A. F. van der Steen, H. J. Vos, M. Versluis and N. De Jong, *Ultrasound Med. Biol.*, 2014, **40**, 1834.
- 6 P. Marmottant and S. Hilgenfeldt, *Nature*, 2003, **423**, 153.
- 7 C. H. Fan, C. Y. Ting, H. L. Liu, C. Y. Huang, H. Y. Hsieh, T. C. Yen, K. C. Wei and C. K. Yeh, *Biomaterials*, 2013, **34**, 2142.

- 8 C. Y. Lai, B. Z. Fite and K. W. Ferrara, *Front. Oncol.*, 2013, **3**, 204.
- 9 W. Xie, S. Liu, H. Su, Z. Wang, Y. Zheng and Y. Fu, *Acad. Radiol.*, 2010, **17**, 1242.
- 10 J. H. Hwang, J. Tu, A. A. Brayman, T. J. Matula and L. A. Crum, *Ultrasound Med. Biol.*, 2006, **32**, 1611.
- 11 C. H. Fan, H. L. Liu, C. Y. Huang, Y. J. Ma, T. C. Yen and C. K. Yeh, *Ultrasound Med. Biol.*, 2012, **38**, 1372.
- 12 Y. Hu, J. M. Wan and A. C. Yu, *Ultrasound Med. Biol.*, 2013, **39**, 2393.
- 13 J. E. Chomas, P. Dayton, D. May and K. Ferrara, *J. Biomed. Opt.*, 2001, **6**, 141.
- 14 D. E. Kruse and K. W. Ferrara, *IEEE Trans. Ultrason. Ferroelectr. Freq. Control*, 2005, **52**, 1320.
- 15 Y. S. Tung, F. Vlachos, J. J. Choi, T. Deffieux, K. Selert and E. E. Konofagou, *Phys. Med. Biol.*, 2010, **55**, 6141.
- 16 N. Wallace, S. Dicker, P. Lewin and S. P. Wrenn, *Ultrasonics*, 2015, **58**, 67.
- 17 M. J. Hsu, M. Eghtedari, A. P. Goodwin, D. J. Hall, R. F. Mattrey and S. C. Esener, *J. Biomed. Opt.*, 2011, **16**, 067002.
- 18 M. A. Nakatsuka, J. H. Lee, E. Nakayama, A. M. Hung, M. J. Hsu, R. F. Mattrey, S. C. Esener, J. N. Cha and A. P. Goodwin, *Soft Matter*, 2011, **2011**, 1656.
- 19 S. M. van der Meer, B. Dollet, M. M. Voormolen, C. T. Chin, A. Bouakaz, N. de Jong, M. Versluis and D. Lohse, *The J. Acoust. Soc. Am.*, 2007, **121**, 648.
- 20 S. P. Wrenn, S. M. Dicker, E. F. Small, N. R. Dan, M. Mleczko, G. Schmitz and P. A. Lewin, *Theranostics*, 2012, **2**, 1140.
- 21 R. H. Abou-Saleh, M. Swain, S. D. Evans and N. H. Thomson, *Langmuir*, 2014, **30**, 5557.
- 22 M. S. Mufamadi, V. Pillay, Y. E. Choonara, L. C. Du Toit, G. Modi, D. Naidoo and V. M. Ndesendo, *J. Drug Deliv.*, 2011, **2011**, 939851.
- 23 K. Johnston, C. Tapia-Siles, B. Gerold, M. Postema, S. Cochran, A. Cuschieri and P. Prentice, *Ultrasonics*, 2014, **54**, 2151.

## Graphical Abstract



A lipid-polymer composite structure was developed for tuning of inertial cavitation activity of microbubbles under ultrasound exposure. The incorporation of a thin layer of polymer networks inside the lipid monolayer resulted in marked reduction in inertial cavitation dose. This strategy is potential to increase the safety of ultrasound theranostic applications assisted by microbubble cavitation.